Indian Journal of Fibre & Textile Research
Vol. 47, September 2022, pp. 334-343
DOI: 10.56042/ijftr.v47i3.45651

Sound absorption characteristics of nanofibre web coated foams

Gamze D Tetik[1,a], Fulya Yilmaz[2] & Gizem Celep[3]

[1]Department of Materials Science and Nanotechnology Engineering, Faculty of Engineering,

[2]Department of Textile Engineering, Graduate Education Institute,

[3]Department of Occupational Health and Safety, Faculty of Health Sciences, Usak University, Usak, Turkey

Received 29 January 2021; revised received and accepted 10 November 2021

Sound absorption properties of polyamide 6 (PA6) nanofibre webs and a widely used sound absorption foam coated with nanofibre webs have been investigated. Initial studies have focused on the electrospinning by using PA6 polymer to obtain uniform and bead-free nanofibres. Thereafter, nanofibres are electrospun on an absorption foam through two spinning durations of 10 h and 20 h. Thicknesses, mass per unit area values, porosities, pore sizes, and Brunauer-Emmet-Teller surface areas of the webs are determined. At characterization stage, sound absorption coefficients of pure nanofibre webs, pure foam, and foams enhanced with nanofibre webs are measured by acoustic impedance tube method. Noise reduction coefficients (NRC) are also calculated. Sound absorption coefficients at 6400 Hz are observed as 0.76 and 0.74 for nanofibre webs electrospun during 10 h and 20 h respectively. The NRC values are found as 0.189, 0.197 and 0.192 for pure foam sample and nanofibre webs electrospun during 10 h and 20 h respectively. Overall results of the study indicate that moderate mid-high frequency sound absorption and noise reduction coefficients are obtained by using the nanofibre web coated foams.

Keywords: Electrospinning, Nanofibres, Noise reduction coefficient, Polyamide 6, Sound absorption, Sound absorption coefficient

1 Introduction

Currently noise is a major environmental problem. Noise, defined as unwanted sound in the workplace, has increased with the development of technology. Sound from different sources, such as traffic, construction, every type of machinery and equipment used in workplace, and air conditioners may have adverse effects on human health in case of long term exposure[1, 2]. To eliminate these effects various sound absorbing materials have been developed by researchers since 1970s[3]. Healthy human ear can hear sounds in the frequency range of 20-20000 Hz. Sound frequencies below 250 Hz are classified in low frequency range. Jet engines, horns, and sirens create sounds in 315-6300 Hz, 300-4000 Hz, and 500-1200 Hz frequency ranges respectively and hence are the examples of mid-high frequency sounds[4].

Sound absorbers are generally categorized into three groups, namely porous, resonance, and other absorbers[5]. Mineral wool, foams, textiles, and fleece are some examples of porous absorbers; flexible sheets and cavity absorbers are the types of resonance absorbers[6, 7]. The basic characteristic of porous absorbers is their open structure that allows motion of sound waves in these gaps. The air molecules present in these gaps of the porous materials create friction forces against sound waves. When these materials absorb sound, sound energy is converted into thermal energy due to their high surface area[6].

It is difficult to absorb low-frequency noise with porous materials since they have more possibility to reach ear due to their inherent paths. Irrespective of low or high frequency sounds, the sound absorption ability of a material is affected by fibre size, flow resistance, porosity, tortuosity, thickness, density, and surface impedance[8]. The properties listed here are considered for nanomaterials. Nanofibres are classified as a type of one-dimensional nanomaterials, considering dimensionality and degree of freedom. Nanofibres have high aspect ratio values and they are produced by various techniques. Electrospinning, centrifugal spinning, template synthesis, and self-assembly of nanofibres were studied for various applications that are quite different from each other. Some of these applications are cosmetics, filtration, sensors, textiles, and sound absorption. The sound absorption is one of the new applications of nanofibre webs. Fine fibre size below 1 μm is one of the basic characteristics of nanofibres. As some researchers

[a]Corresponding author.
E-mail: gamze.tetik@usak.edu.tr

emphasized, an increase in the number of fine fibres in sound absorption materials led to an increase in the possibility of sound waves to encounter with these fine unit structures[9, 10]. Flow resistance is supplied by the entangled fibres in nonwovens. They serve as obstacles in front of moving sound waves[8]. Besides, Seddeq[8] stressed that as the fibre diameter decrease, the flow resistance per unit thickness increase for a constant porosity. The frictional losses are provided by gaps in porous materials. Sound waves that easily penetrate to the pores of these materials oscillate and show loss of momentum occurred by means of the flow of sound waves through irregularly distributed pores. Thus, the sound absorption materials that are more porous exhibit better sound absorption property[11]. Parallel arrangement of nanofibres in the web is a factor reducing the friction of sound waves. Pores created by more entangled nanofibre web structures are more successful in converting sound energy to mechanical and heat energy[12]. Improvement in the sound absorption coefficient values was observed by a group[13] in the low and medium frequency range by increasing the thickness values of nanofibre webs. It is known that nanofibres can lead an increase the sound absorption ability without having a great effect on the thickness of the absorption material. Density is another effective factor for sound absorption. Koizumi *et al.*[14] stated that above 1000 Hz, the increase in density of bamboo fibre based absorbent material led sound absorption coefficient to decrease due to the buried cavities by fibres. Finally, surface impedance is a parameter that is related to flow resistance, porosity, tortuosity and thickness of the absorbing material[15]. Moreover, some theoretical modelling studies were conducted to determine surface impedance and to investigate the interactions with sound absorption property[16]. Cao *et al.*[17] studied the determination of surface impedance for nanofibrous aerogels with various thicknesses. They remarked that more sound energy loss and less reflection of sound energy were observed for thicker materials.

Some researchers tried to utilize the advantages of nanofibres in terms of abovementioned properties in sound absorption applications. Bahrambeygi *et al.*[18] investigated a sandwich structure composed of polyurethane (PU) and polyacrylonitrile (PAN) nanofibres with PU foams. They concluded that sandwich structures including PAN and PU nanofibre layers resulted in an increase in sound absorption coefficients at a frequency range of 100-6300 Hz. Another group[19] studied acoustical properties of polyvinyl pyrrolidone (PVP), polystyrene, and polyvinyl chloride electrospun https://www.britannica.com/science/polyvinyl-chlori-denanofibres for noise reduction in aircrafts. According to their results, electrospun nanofibres absorb sound at higher frequencies depending on fibre type, weight, and thickness. Comparisons of sound absorptions of multiple layers of nanofibre webs and microfibre fabrics has been studied by Na *et al.*[20]. They studied suede, mesh, terry, and queenscord microfibre fabrics. They plied nanofibre layers and obtained multilayered nanofibre fabrics with similar weights to microfibre ones. They claimed better sound absorption results from multiple nanofibre webs in the frequency range of 1000-4000 Hz. Rabbi *et al.*[21] investigated PU and PAN nanofibres incorporated into polyester and wool-based nonwovens. They examined sound transmission loss and sound absorption properties of these nonwovens. Nanofibre incorporation improved both properties at low and middle frequencies. PA6 nanofibres used with foam, felt and kenaf were also studied by Trematerra *et al.*[22]. They deduced that the results of the foam and felt with nanofibres were good in the range of low and middle frequencies, and the result of the kenaf with nanofibres was good at high frequencies. For the investigation of sound absorption properties, warp knitted spacer fabrics were coated with nanofibres as well as foams. Researchers[23] stated that there was an improvement in the sound absorption ability of the fabrics without any significant thickness and weight increase.

In order to determine the sound absorption properties of PU foams that are widely used in sound absorption applications, we designed PU foams coated with PA6 nanofibre webs via two electrospinning durations. Subsequently, sound absorption coefficients were measured by impedance test tube method and the noise reduction coefficients were calculated.

2 Materials and Methods

2.1 Materials

PA6 and formic acid (FA) were chosen as polymer and solvent respectively for producing nanofibres, as PA6/FA polymer solution is easily electrospinnable. They both were purchased from Sigma-Aldrich (Steinheim, Germany). Molecular weight of the PA6 polymer is 10000 g/mol, melting temperature is 228.5 °C, and the density of the polymer at 25 °C is 1.084 g/mL.

The 98-100 % pure formic acid having a density of 1.22 g/mL at 25 °C was also used. Homogenous electrospinning solutions were obtained by stirring on a magnetic stirrer for 24 h at 20±2 °C. A high voltage power supply (Gamma, ES50P10W/DAM, Gamma High Voltage, Ormond Beach, FL, USA) and a syringe pump (NE1000, New Era Syringe Pump Systems Inc., Farmingdale, NY, USA) were used during electrospinning. The polymer solution was fed via 20 mL plastic syringe placed on the syringe pump. A 21 gauge stainless steel needle cut to a length of 25 mm was also used as spinneret. Aluminium foil coated stationary metal plate was used as collector during preliminary studies. Grounding was performed by attaching a crocodile clips to this collector. In order to achieve the coating on foam sample, the back side of the foam was taped with an Al conductive band and attached on the collector to guarantee the electrical field stability (Fig.1); conductive Al or copper bands have also been used in previous studies for this purpose[24-26].

PU foam sample was kindly provided from a local company (Dinamik Yalıtım Malz. Industry and Trade Inc, Turkey). The physical properties of this foam sample were indicated as follows by the producer: 15±2 mm thickness, 83 kg/m^3 density, and 50 kPa tensile strength.

2.2 Methods

2.2.1 Electrospinning Parameters

Eight different preliminary electrospinnings were performed with two concentrations (15 % and 20 % w/v), two applied voltages (22 kV and 26 kV) and two distance (15 cm and 20 cm) values to determine the optimum PA6 nanofibre production parameters. The flow rate was adjusted at 4 µL/min. These parameters were determined by considering the straight section of the stable jet that was visible by naked eye. The electrospinnings were performed at 20±2 °C.

Preliminary studies included the determination of optimum parameters for uniform and bead-free nanofibres. After morphological analysis, duration of electrospinning was changed since it affected the thickness of the nanofibre web. Thickness is a major parameter that influences sound absorption properties, so 10 h and 20 h of single jet electrospinnings were performed with same parameters both on PU foams (Fig. 1) and Al foil. Characterizations related to sound absorption were performed with the non-coated and the PA6 nanofibre coated foam samples. All other tests were carried out using pure PA6 nanofibre webs. Thicknesses of these webs were measured by a micrometer (Mitutoyo, Japan) with an accuracy of 10 µm and also mass per unit area values were determined using an analytical balance (Radwag, Radom, Poland) with an accuracy of 0.1 mg. The samples were coded as in Table 1 for the ease of expression. Thickness and mass per unit area values are given in Table 2. The additional thickness and weight of the nanofibre webs were inconsequential when compared to the 15 mm thick PU foam.

2.2.2 Morphological and Topographical Analyses

Scanning electron microscopic (SEM) and atomic force microscopic (AFM) images were taken with LEO 1430 VP SEM (Leo Electron Microscopy Ltd., Cambridge, UK) and AFM Workshop (CA, USA) respectively for morphological and topographical analysis of nanofibre webs. Acceleration voltage was adjusted as 20 kV in SEM instrument and the samples, created with 5 min electrospinning durations, were gold sputtered before analyses. Means and standard deviations of fibre diameters were determined by measuring 100 fibres randomly chosen

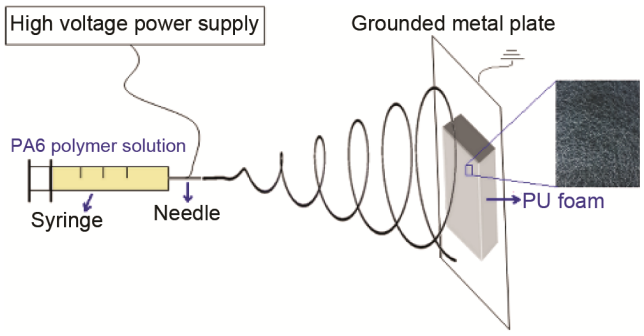

Fig. 1 — Schematic view of electrospinning on PU foam

Table 1 — Codes of samples

Codes	Samples
10h-web	Nanofibre web electrospun during 10 h
20h-web	Nanofibre web electrospun during 20 h
10h-wf	Foam coated with nanofibre during 10 h
20h-wf	Foam coated with nanofibre during 20 h
Pure-f	Pure foam sample

Table 2 — Thickness and mass per unit area values of electrospun nanofibre webs

Codes	Electrospinning duration, h	Thickness µm	Mass per unit area, g/m^2
10h-web	10	50±8	5.43±1.41
20h-web	20	100 ±12	12.26±3.56

from SEM images by means of ImageJ measurement and visualization software. 3D AFM images of the PA6 nanofibre webs electrospun during 10 h and 20 h were taken with scan size of 10 µm x 10 µm for topographical analyses. AFM images were investigated by Gwyddion which is a data visualization and analysis program for scanning probe microscopes. In this way, average surface roughness (r_a), root mean square (rms), surface skewness (R_{sk}) and coefficient of kurtosis (R_{ku}) values of nanofibre webs were determined.

2.2.3 Measurement of Porosity and BET Surface Area

Porosity and pore size distributions of nanofibre webs electrospun during 10 h and 20 h were determined by a mercury intrusion porosimetry (Autopore IV 9500, Micromeritics, USA). Nanofibre webs provide increased porosity, low pore sizes and low pore size distributions that are remarkable in terms of sound absorption properties. So, it is clear that the measurement of porosity and pore sizes are necessary. Mercury intrusion porosimetry tests were performed both with PU foam and nanofibre webs according to the ASTM UOP578-11 test standard.

Brunauer-Emmett-Teller (BET) surface area measurements were performed by means of a Micromeritics Gemini 2380 analyzer (Norcross, GA, USA). Samples were degassed at 100 °C for 1 h and then measurements of BET surface areas of the samples were carried out by physical adsorption and desorption of nitrogen gas according to the ISO 9277:2010 test standard. Since many improved properties of the nanofibre webs depend on the increased surface area of them when compared to microfibre webs, the measurement of the BET surface area of nanofibre webs is required. Surface area of a nanofibre web is closely related to the basic desired property that may differ in accordance with the application. Increased surface area of the nanofibre web means that there is a large contact area created between the surface of the web and the environmental components. The effects of the increased contact area between the surface of the webs and the sound transferring on these surfaces were examined.

2.2.4 Measurement of Sound Absorption Coefficients

Sound absorption coefficient measurements were performed by acoustic impedance test tube method in the 110-6400 Hz frequency range according to the ISO 10534-2 standard. Figure 2 shows the experimental set up (TestSens, Bias, Turkey) of the method. For the measurement of the sound absorption coefficient, the characteristic sound signal is produced by software of the instrument, amplified and send to the chamber as sound wave (Fig. 2). There is a non-permeable lid used as terminator at the end of the chamber. The microphones 1 and 2 measure the pressure values formed by sound waves. These two values are proportioned to calculate reflectance coefficient. The reflectance coefficient is related to SAC which takes values between 0 (no absorption) and 1 (perfect absorption) by the software of the instrument.

Results of the tests were considered in four categories, viz low (110-250 Hz), low-middle (mid) (250-500 Hz), mid (500-1600 Hz), and mid-high (1600-6400 Hz) frequency ranges. The samples sizes for low, low-mid, and mid frequency ranges were 100.5 mm and the sample sizes for mid-high frequency ranges were 29.5 mm. Five measurements were taken for all the ranges tested and the graphs were created by using mean values. The statistical analyses were performed by IBM SPSS 23. The effects of material types on SAC values at 250 Hz (low), 500 Hz (low-mid), 1000 Hz (mid), and 6400 Hz (mid-high) were analyzed using the One-Way analysis of variances test, and homogeneities of variances were tested with Levene's test. The Tukey or Tamhane's T2 tests were used for homogeneous or non-homogeneous variances respectively. The p value of 0.05 was accepted as significant. Noise reduction coefficients (NRC) of all samples were also calculated as reported earlier[26]. The arithmetic mean of the SAC values at frequencies of 250, 500, 1000, 2000, and 4000 Hz were included in the calculation of NRC for each sample. The samples were coded as shown in Table 1.

3 Results and Discussion

3.1 Electrospinning Results

The SEM images of the nanofibre webs produced with the determined concentrations (C), applied voltages (V), and distances (D) are given in Fig. 3.

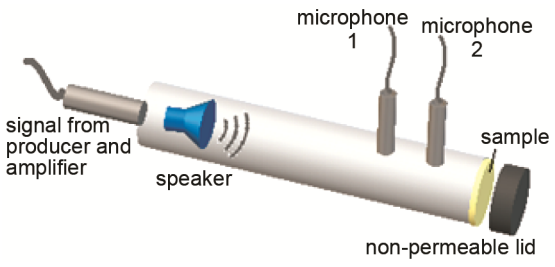

Fig. 2 — Schematic view of sound absorption coefficient measurement set- up

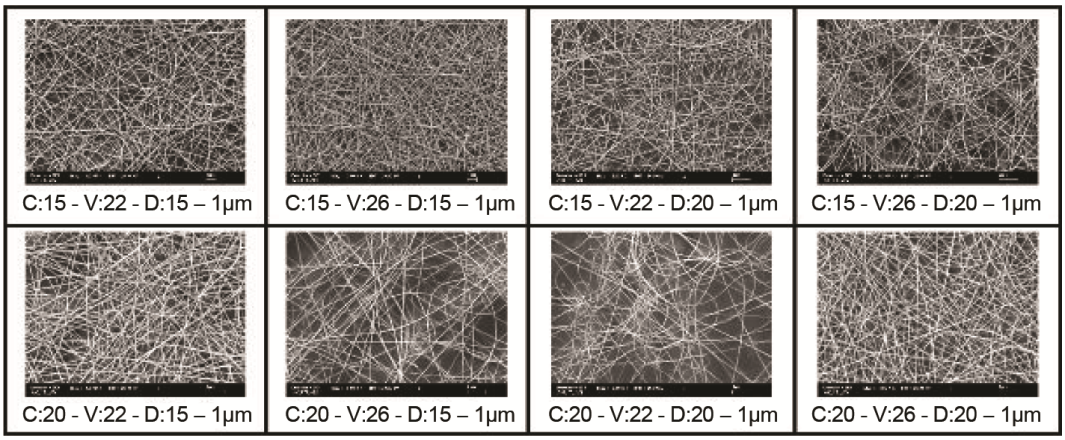

Fig. 3 — SEM images of nanofibre webs produced (magnification: KX 5.00)

SEM images show bead-free and uniform nanofibres. Since PA6 polymer is an easily electrospinnable one, homogenous nanofibres are obtained. Means and standard deviations of fibre diameters are given in Table 3. Keeping all other parameters at constant levels, mean fibre diameter is found to decrease with increasing distance. This can be attributed to the increase in the flight time of the polymer jet and also the electrostatic forces acting on the jet. Same tendency was observed for applied voltage since it directly forms the electrostatic forces. The increase in the concentration of solution means more viscous drag forces acting against electrostatic forces and so higher mean fibre diameters are observed with 20% w/v than with 15 % w/v.

Since none of the nanofibres is found beaded and non-uniform, the minimum fibre diameter and diameter distribution are selected for long term electrospinning (26 kV, 15% w/v, and 20 cm). Figure 4 shows the SEM images of non-coated and coated PU foams. While open structured pores of non-coated PU foam can be seen in Fig. 4 (a), SEM images taken after 5 min electrospinning can be seen in Fig. 4 (b). SEM images prove the formation of uniform and beadless nanofibres on the foam surface.

Table 3 — Mean fibre diameters obtained with parameters

Concentration %	Applied voltage, kV	Distance cm	Mean fibre diameter, nm	Std. deviation nm
15	22	15	119.93	11.51
15	22	20	94.52	11.63
15	26	15	101.03	11.72
15	26	20	84.60	7.95
20	22	15	122.27	7.83
20	22	20	118.49	7.11
20	26	15	111.39	11.36
20	26	20	101.98	11.52

Table 4 — Average surface roughness (r_a), root mean square (rms), surface skewness (R_{sk}) and coefficient of kurtosis (R_{ku}) values of electrospun webs

Samples	r_a, nnm	rms, nm	R_{sk}	R_{ku}
10h-web	37.68	49.70	0.36	0.47
20h-web	16.99	21.52	0.39	-0.03

3.2 Topographical Analyses

AFM images of the 10h-web and 20h-web are given in Figs. 5 (a)-(f). The r_a, rms, R_{sk}, and R_{ku} values of both electrospun webs calculated are given in Table 4.

AFM images and the calculations made on them exhibit that average surface roughness values of nanofibre webs are approx. 38 nm and 17 nm for 10 h and 20 h electrospinning durations respectively. Rms values that show the change in surface roughness are determined as 49.7 nm and 21.5 nm for 10h-web and 20h-web respectively. Rms values are lower than average fibre diameter because of the close-packed structure of nanofibre webs according to long-time electrospinning. The increase in the electrospinning duration decreases the rms value 2.3 times. It indicates that a dense structure with increasing duration is formed. The surface of the 20h-web is found flattened during electrospinning in accordance with the accumulation of the fine fibres and a compact structure is obtained, as reported earlier[26].

Symmetry of surface height distribution, determined by R_{sk}. R_{sk} values of the both webs, are found close to each other and zero. This means surface height distribution is close to normal distribution[27]. R_{sk} value is also related to the wholeness of the webs. It represents that there are more areas where the surface heights of the webs are below the mean value, since both of the R_{sk} values are positive.

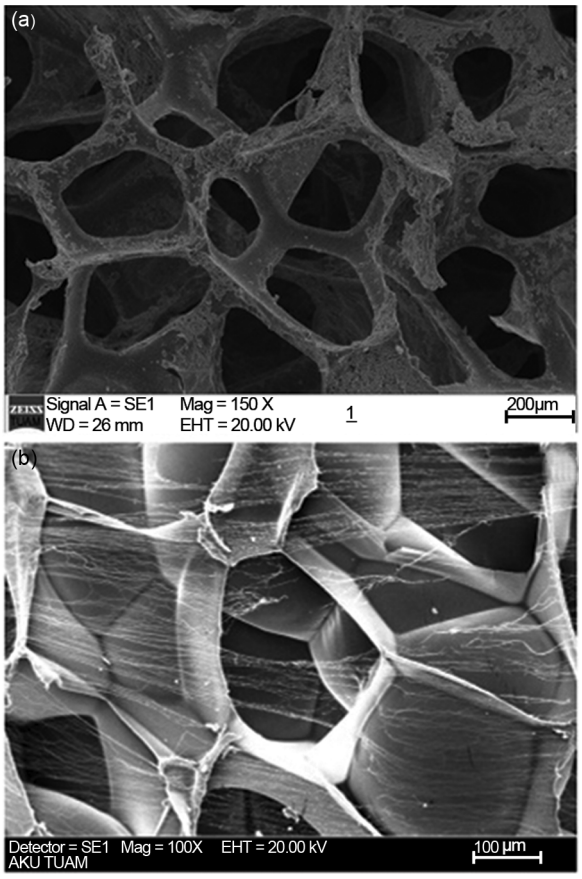

Fig. 4 — SEM images of (a) non-coated PU foam (mag: ×150) and (b) PA6 nanofibres electrospun on PU foam for 5 min (mag: ×100)

R_{ku} value gives insight to the shapes of peaks on the nanofibre web. While a positive R_{ku} is a sign of sharp peaks (spiky structured), a negative one exhibits flat peaks on the surface of the web (bumpy structured)[27-29]. 10h-web has a positive R_{ku} demonstrating sharp peaks on the web, while 20h-web has a negative value indicating flat peaks on the surface of the web. As the web density is increased with increasing electrospinning duration, flattening of the structure occurs, showing the compactness of the structure.

3.3 BET Surface Area and Porosity

BET surface areas of the 10h-web and 20h-web are measured as 98.36 and 75.95 m^2/g respectively. Average pore volume (APV) and average pore diameter (APD) values are also calculated by the software of the instrument. Values of 0.14 cm^3/g for APV and 4.43 nm for APD are observed for 10h-web. APV and APD values for 20h-web are observed as 0.12 cm^3/g and 4.21 nm respectively. The difference in the observed values for the samples originates from the morphological and structural changes. The total number of fine fibres and overlaps of these fibres increase with electrospinning duration and these make the web dense and thick. Since the 20h-web is denser and thicker than the 10h-web, BET surface area is decreased approx. 23%, as also supported by the literature[30]. The increase in the density of nanofibre

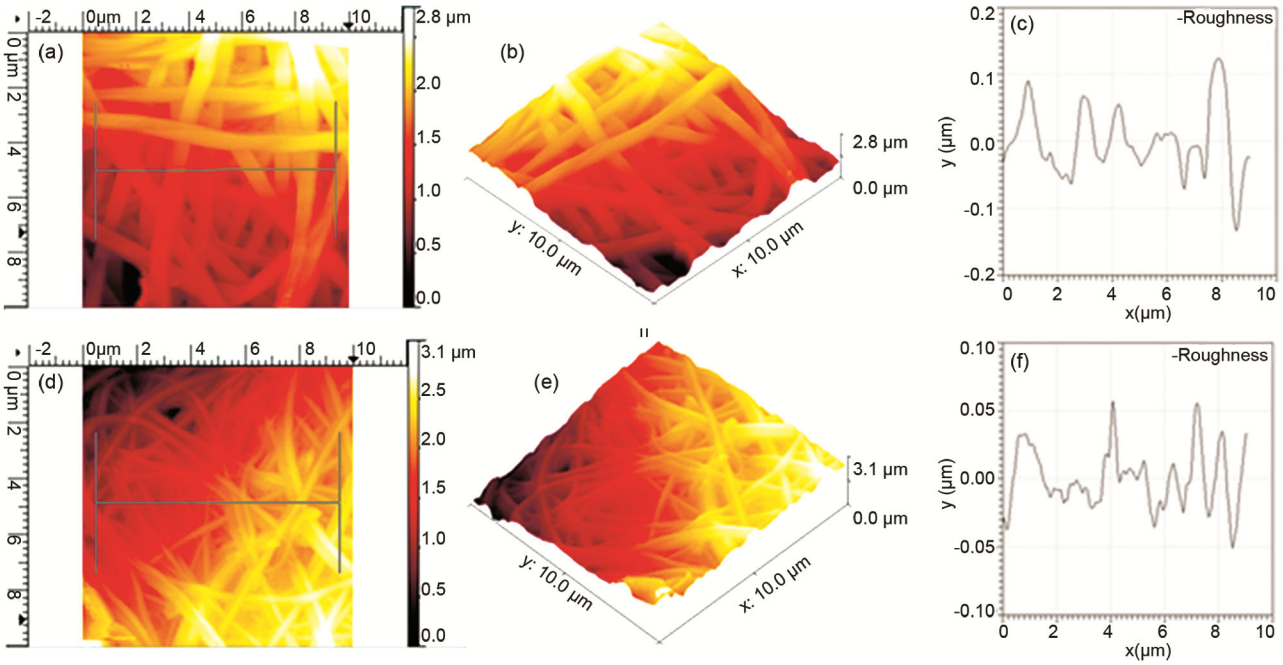

Fig. 5 — AFM images of nanofibre web electrospun (a, d) 2D AFM image and height diagram, (b, e) 3D AFM image, and (c, f) distribution of roughness during 10 h and 20 h respectively

webs means an increase in the fibre mass and the number of fibres in the unit volume[31]. This results in the creation of more intersections between these fibres. Thus, high density of nanofibre webs leads to a decrease in pore sizes[32, 33]. Hence, an increase in the spinning duration leads to an increase in the density and a decrease in the pore diameter in this study.

These results are consistent with the porosimetry results as can be seen from Table 5. Although BET surface area instrument gives an APD value, valid APD values can be measured by porosimetry instrument.

As seen from Table 5, the bulk density of the 20h-web is more than that of the 10h-web. Denser web obtained with long electrospinning duration has lower pore sizes and lower porosity than loose and thin nanofibre web. As stated in AFM results, the compactness and closely packed structure of the 20h-web is responsible for this phenomenon[34, 35]. Electrospinning duration increase leads to total porosity decrease from approx. 87% to 80%. In addition, the variation in the APD values (volume, area, and 4V/A) asserts the observation of very wide ranged pore size distribution in both nanofibre web samples[36].

Total porosity of the foam is measured as approx. 46%. Its bulk density (0.88 g/mL) is found much higher than nanofibre webs. Pores of the foam sample are found wide, as seen from the SEM images.

3.4 Sound Absorption Tests

Sound absorption coefficient graphs are shown in Figs 6 (a)-(d) for low (110-250 Hz), low-mid (250-500 Hz), mid (500-1600 Hz), and mid-high (1600-6400 Hz) frequency ranges respectively.

According to the statistical analyses, SAC values of the pure nanofibre webs recorded at 200 Hz are significantly different from coated and non-coated foam samples ($p<0.05$). SAC values of pure nanofibre webs are lower [Fig. 6(a)]. This effect may be due to the low thicknesses of pure nanofibre webs. They can be considered as insufficient in sound absorption when used alone. When low-mid (500 Hz) frequency analysis is evaluated, it represents that SAC values of all samples are significantly different from each other, except 20h-wf and pure-f ($p=0.867$). The coated and non-coated foam samples exhibit higher SAC values than pure nanofibre webs at this frequency [Fig. 6(b)]. It is reported[23] that fine fibres and high surface area of nanofibre webs enhance sound absorption in low and mid frequency ranges. The low SAC values obtained at low and mid frequencies can be related to the surface density (g/m^2 in units and called as mass per unit area in this study) of nanofibre webs[37]. It

Table 5 — Mercury porosimeter results
[Stem volumes used: 37-53 % for all the samples tested]

Samples	Total intrusion volume, mL/g	Total pore area m^2/g	Average pore diameter, nm			Bulk density g/mL	Porosity %
			Volume	Area	4V/A		
10h-web	15.52	99.95	73231.3	84.5	621.0	0.06	87.34
20h-web	6.22	54.63	3372.2	44.4	455.2	0.13	79.84
Pure foam	0.52	0.49	70049.5	728.1	4220.3	0.88	45.76

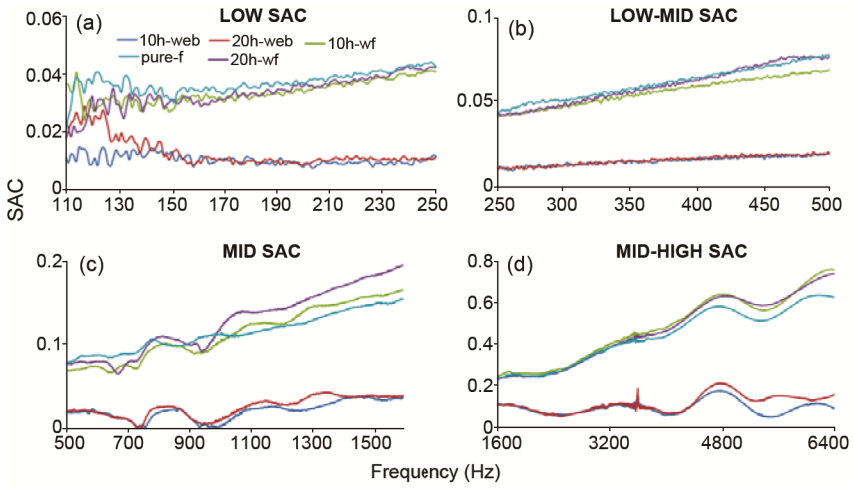

Fig. 6 — SAC values of samples at (a) low frequency, (b) low-mid frequency, (c) mid frequency and (d) mid-high frequency ranges

represents that the mass per unit area values of pure nanofibre webs are too low to create an increase in SAC values at low and low-mid frequencies. Tukey multiple comparison test results conducted at 1000 Hz show that differences between 10h-wf and 20h-wf samples, and 10h-wf and pure-f samples are not statistically significant ($p=0.827$ and $p=0.281$ respectively). The SAC values of all samples recorded at 1000 Hz have similar tendencies to the values recorded at 500 Hz [Figs 6(b) and (c)].

At mid-high frequency ranges [Fig. 6(d)], nanofibre web coating increases the sound absorption coefficient of the foam. The SAC value of the pure foam is raised from 0.62 to 0.76 and 0.74 at 6400 Hz for 10h and 20h electrospinning respectively. These values are significantly different from pure-f, 10h-web, and 20h-web. 10h-wf and 20h-wf samples are not found statistically different from each other ($p=0.892$). In summary, the SAC value of pure foam is increased by 22.6% and 19.3% with coatings of 10 h and 20 h electrospinning respectively. However, these small increases in SAC values are not high enough to make the nanofibre web coated foam to be used as effective sound absorbers. Although nanofibre webs with high porosity and low pore diameters are given in the class of porous media in some studies on sound absorption; there are studies in which sound absorption materials are considered as resonance absorbers[38, 39]. In the later studies, it is stated that the contribution made on the sound absorption coefficients depends on the absorption created by the heavily vibration of nanofibre membranes at the resonance frequencies and converting sound energy to heat energy by means of this vibration[40]. The small increases in the SAC values of the nanofibre web coated foams can be related to this phenomenon. The nanofibre webs vibrating during the measurements at mid-high frequencies presumably cause a combined effect with the pure foam structured porous media.

The SAC values used in the calculation of NRC values are given in Table 6. According to the NRC results, it can be summarized that sound absorption ability of the foam is slightly increased approx. 4.2% and 1.6% by electrospun nanofibre coatings during 10 h and 20 h respectively. This increase can be attributed to the randomly arranged fine fibre structure of the nanofibre webs coated on the foam during long electrospinning durations. The fine fibre diameters obtained in the range of 80-90 nm (Table 3) play a significant role in this case. Since SAC is the ratio of the acoustic energy absorbed by the material to incident energy, the SAC value is raised by the absorption of incident sound through the structure having little pores and high porosity. Smaller pores and higher porosity of the porous sound absorption materials results in more sound energy loss due to frictional forces. This is provided by the nanofibre web coatings with pores as low as 84 nm and 44 nm and porosities as high as 87 % and 80 % (Table 5), for the 10h-web and 20h-web respectively. Besides, increased surface area contributes to this phenomenon by the creation of more frictional areas on the surface of the webs. BET surface areas of the 10h-web and 20h-web are approx. 98 m^2/g and 76 m^2/g respectively, and it is possible to say that these values can easily be obtained by needle electrospinning method. Further, it is believed that the low densities of nanofibre webs contribute to the increase in sound absorption ability.

It is obvious that surface roughness values of the nanofibre webs are lower than the micro-structured porous materials[41]. In this study, it was observed that the nanofibre web coated foam samples exhibiting low average roughness values result in high sound absorption coefficients. These results are contradictory to earlier works. Sung *et al.*[42] studied the open pore structured foams and obtained the highest sound absorption coefficient in the foam, exhibiting the maximum average roughness value, and low coefficients for the structures possessing roughness below this value. It can be summarized that the potential effect of roughness may be suppressed by other properties obtained via nanofibres, such as high porosity, high surface area, and low density.

Table 6 — SAC values of samples used in NRC calculation

Samples	SAC values (10^{-3}) at different frequencies					NRC
	250 Hz	500 Hz	1000 Hz	2000 Hz	4000 Hz	
10h-web	11.0±1.5	19.0±1.0	48.0±1.0	91.0±1.0	62.0±1.0	0.046
20h-web	12.0±1.5	20.0±2.0	54.0±2.0	98.0±7.0	71.0±0.4	0.051
10h-wf	41.0±0.6	69.0±1.0	133.0±5.0	261.0±16.0	481.0±4.0	0.197
20h-wf	43.0±0.4	77.0±1.0	132.0±2.0	245.0±14.0	464.0±1.0	0.192
Pure-f	42.0±0.8	78.0±2.0	135.0±2.0	248.0±13.0	440.0±2.0	0.189

4 Conclusion

In this study, PA6 polymer nanofibre webs have been electrospun during long durations both as pure webs and on PU foam. Fine, uniform and beadless fibres ranging between 80 nm and 90 nm are obtained. According to the analyses, nanofibre webs possessing thicknesses of 50 µm and 100 µm, mass per unit area values of 5.5 g/m^2 and 12.0 g/m^2, porosities of 87% and 80%, average pore diameters of 621 nm and 455 nm, surface areas of 98 m^2/g and 76 m^2/g, bulk densities of 0.06 g/mL and 0.13 g/mL, and average roughness of 38 nm and 17 nm are obtained for 10 h and 20 h electrospinning durations respectively. All these nanofibre characteristics affect the sound absorption property of the foam coated with nanofibre webs. Impedance test tube measurements exhibit that the sound absorption and noise reduction coefficients of the nanofibre web coated foams are moderate at mid-high (1600-6400 Hz) frequency range. Since statistical analyses show that there are no significant difference in the SAC values of the nanofibre webs obtained by 10 h and 20 h of electrospinning at 6400 Hz, it can be concluded that nanofibre web coatings on foam increase the sound absorption coefficients by approx. 20%. The calculated NRC values demonstrate that nanofibre web coating slightly increases the noise reduction.

The overall results obtained in this study clearly show that in further studies, materials having high sound absorption coefficients can be coated by nanofibre webs with short electrospinning durations in order to obtain efficient sound absorbers. In this way, sound absorption materials with higher average surface roughness values and low densities can be produced to contribute the sound absorption ability avoiding creation of buried cavities of fibres on the webs.

Acknowledgement

The authors thankfully acknowledge the Usak University Scientific Research Coordination Unit for their support (Grant No. 2015/MF003).

References

1 Talukdar M K, *Indian J Fibre Text Res*, 26 (2001) 44.
2 van Kempen E, Fischer P, Janssen N, Houthuijs D, van Kamp I, Stansfeld S & Cassee F, *Environ Res*, 115 (2012) 18.
3 Arenas J P & Crocker M J, *Sound Vib*, 44 (2010) 12.
4 Konopka W, Pawlaczyk-Luszczńska M & Śliwińska-Kowalska M, *Med Pr*, 65 (2014) 583.
5 Cox T & D'antonio P, *Acoustic Absorbers and Diffusers: Theory, Design and Application* (Boca Raton: Taylor & Francis), 2016, 575.
6 Jacobsen F, Poulsen T, Rindel J H, Gade A C & Ohlrich M, *Fundamentals of Acoustics and Noise Control* (Technical University of Denmark), 2011, 172.
7 Zainulabidin M, Rani M A, Nezere N & Tobi A L M, *Int J Mech & Mechatron Eng,* 14 (2014) 118.
8 Seddeq H S, *Aust J Basic Appl Sci,* 3 (2009) 4610.
9 Lee Y Joo C, *Autex Res J,* 3 (2003) 78.
10 Kucukali-Ozturk M, Nergis B & Candan C, *J Ind Text*, 47 (2018) 1739.
11 Bihola D V, Amin H N & Shah V D, *Int J Eng Sci Futur Tech*, 1 (2015) 1.
12 Gao B, Zuo L & Zuo B, *Fiber Polym*, 17 (2016) 1090.
13 Xiang H F, Tan S X, Yu X L, Long Y H, Zhang X L, Zhao N & Xu J, *Chin J Polym Sci,* 29 (2011) 650.
14 Koizumi T, Tsujiuchi N & Adachi A, *High Performance Structures and Composites* (WIT Press, Southampton), 2002, 157.
15 Carpinello S, L'Hermite P, Bérengier M & Licitra G, *Radiat Prot Dosim*, 111 (2004) 363.
16 Takahashi Y, Otsuru T & Tomiku R, *Appl Acoust*, 66 (2005) 845.
17 Cao L, Si Y, Wu Y, Wang X, Yu J & Ding B, *Nanoscale,* 11(5) (2019) 2289.
18 Bahrambeygi H, Sabetzadeh N, Rabbi A, Nasouri K, Shoushtari A M & Babaei M R, *J Polym Res*, 20 (2013) 1.
19 Khan W S, Asmatulu R & Yildirim M B, *J Aerospace Eng*, 25 (2012) 376.
20 Na Y, Agnhage T & Cho G, *Fiber Polym,* 13 (2012) 1348.
21 Rabbi A, Bahrambeygi H, Shoushtari A M & Nasouri K, *J Eng Fiber Fabic,* 8 (2013) 36.
22 Trematerra A, Iannace G, Nesti S, Fatarella E & Peruzzi F, *International Conference*, *7th Forum Acusticum*, (Krakow), 7-12 September 2014.
23 Kucukali-Ozturk M, Ozden-Yenigun E, Nergis B & Candan C, *J Ind Text,* 46 (2017) 1498.
24 Storck JL, Grothe T, Mamun A, Sabantina L, Klöcker M, Blachowicz T & Ehrmann A, *Mater*, 13 (1) (2020) 47.
25 Doğan G, Başal G, Bayraktar O, Ozyildiz F, Uzel A & Erdogan I, *Microsc Res Tech*, 79 (2016) 38.
26 Shahani F, Soltani P & Zarrebini M, *J Eng Fiber Fabr*, 9 (2014) 84.
27 Zhao S, Li Y, Wang Y, Ma Z & Huang X, *Fuel,* 244 (2019) 78.
28 Yudar H H, Pat S, Korkmaz Ş, Ozen S & Senay V, *J Mater Sci: Mater Electron,* 28 (2017) 14499.
29 Kumar B R & Rao T S, *Dig J Nanomater Bios*, 7 (2012) 1881.
30 Jung W H, Kwak N-S, Hwang T S & Yi K, *Appl Surf Sci,* 261 (2012) 343.
31 Lee S & Obendorf SK, *Text Res J*, 77(9) (2007) 696.
32 Thilagavathi N, Muthukumar S, Krishnanan N & Senthilram T, *J Nat Fibers,* 17(10) (2020) 1391.
33 Chiu H T, Lin J M, Cheng T H & Chou S Y, *Express Polym Lett*, 5 (2011) 308.
34 Gu B K, Park S J, Kim M S, Kang C M, Kim J & Kim C H, *Carbohyd Polym*, 97 (2013) 65.
35 Min B-M, Lee G, Kim S H, Lee T S & Park W H, *Biomaterials,* 25 (2004) 1289.
36 Baltieri R C, Innocentini-Mei L H, Tamashiro W, Peres L & Bittencourt E, *Eur Polym J*, 38 (2002) 57.
37 Rabbi A, Bahrambeygi H, Nasouri K, Shoushtari A M & Babaei M R, *Adv Polym Technol*, 33 (2014) 8.

38 Kalinova K, Ozturk M K & Komarek M, *J Text Inst*, 107 (2016) 1068.
39 Mohrova J & Kalinova K, *J Nanomater,* 2 (2012) 4.
40 Kalinova K, *J Nanomater,* 1 (2011) 6.
41 Ura D P, Karbowniczek J E, Szewczyk P K, Metwally S, Kopyściański M & Stachewicz U, *Bioeng,* 6 (2019) 12.
42 Sung G, Kim J S & Kim J H, *Polym Adv Technol*, 29 (2018) 852.